

Simultaneous Isomerization and Etherification of Isoamylenes with Methanol

By Päivi Kiviranta-Pääkkönen* and A. Outi I. Krause

The effect of feed MeOH/2M1B molar ratio on the initial isomerization and etherification rates of 2-methyl-1-butene (2M1B) was studied in a batch reactor. The initial reaction rates for etherification and isomerization increased when the MeOH/2M1B molar ratio decreased. The ratio of etherification and isomerization rate was 2–3 until at lowest initial MeOH/2M1B molar ratio 0.2, where the isomerization rate increased significantly. At MeOH/2M1B molar ratio 0.2 the isomerization reaction rate was twice as high as the etherification reaction rate. Several kinetic formulations were tested to explain this new data and the data obtained in earlier studies. According to the statistics, a kinetic model based on three active sites gave the best fit, but it was discussed that the basic Langmuir-Hinshelwood mechanism might be more adequate. An improved fit of the Langmuir-Hinshelwood model was obtained, when a correction factor describing the acceleration of isomerization rate with the molar fraction of 2M1B was added into the kinetic equations.

1 Introduction

Precise kinetic models are generally valuable in process design, because they are the basis for both feasible and intrinsically cleaner processes. With the aid of the detailed kinetic models the reactors can be designed in an optimal way, e.g., to choose the operating conditions in such way, that the yield of the valuable product is maximized and byproducts minimized. Kinetic models based on reasonable mechanistic knowledge or assumptions are generally preferred over empirical ones, because the scale-up from laboratory to industrial process is on safer ground when a mechanistic model is available.

The reformulated gasoline component TAME (tert-amyl methyl ether, 2-methoxy-2-methylbutane) is synthesized in an acid-catalyzed, equilibrium reaction of isoamylenes (2-methyl-1-butene, 2M1B, and 2-methyl-2-butene, 2M2B) with methanol (MeOH). The networks and nomenclature for the reactions are presented in Fig. 1. The reaction pairs (r1 and r2),

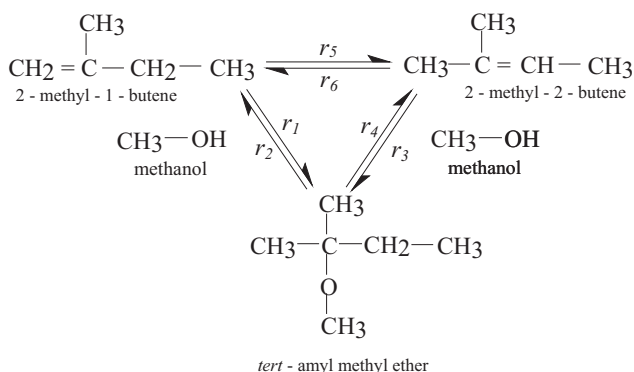


Figure 1. The reaction network for TAME.

(r3 and r4) and (r5 and r6) shown in Fig. 1 establish the reaction equilibrium. When using ion-exchange resins as catalyst and consequently mild temperatures, only alkenes with a double-bonded tertiary carbon atom react in the etherification reaction [1]. From the three isoamylenes, 2-methyl-1-butene reacts fastest and 2-methyl-2-butene is two times slower, when a stoichiometric composition of feed reagents is used [2], whereas 3-methyl-1-butene gives no reaction [1]. In addition to the etherification, the isomerization of the alkene double bond occurs simultaneously. The equilibrium favors more stable 2M2B [3].

The TAME system is complex from the kinetic modeling point of view, as the rate parameters tend to be heavily correlated because the six simultaneous reactions are linearly dependent. However, a proper kinetic model with a correctly predicted reaction equilibrium is essential in the design of etherification process. Moreover, the model should cover a wide range of conditions because in the novel etherification processes, the etherification conversions can be maximized by side reactor configuration or by reactive distillation. Under these conditions, the methanol/isoamylenes ratio can differ greatly from the stoichiometric value [4].

It is a well-recognized fact that both the etherification kinetics and the thermodynamic equilibrium are better described in terms of component activities rather than concentrations [5]. This is because of the sole nature of the reactive system, that is a mixture of polar and non-polar components, and also because of the applied catalyst. Generally, when ion-exchangers are used as a catalyst, significant activity corrections are needed to describe the kinetics, because the exchanger phase can be viewed as forming a nonideal solution [6]. The most widely used activity coefficient method in context with etherification reaction systems has been the well-known group-contribution method UNIFAC, but also UNIQUAC and Wilson-method have been applied. These methods have been widely used in the vapor-liquid equilibrium calculations. Lately, a question has been raised, whether the kinetic models based on activities are able

[*] Lic.Sc.(Tech) P. Kiviranta-Pääkkönen (author to whom correspondence should be addressed, e-mail: Kiviranta@polte.hut.fi), Prof. Dr. (Tech) A. O. I. Krause, Helsinki University of Technology, Laboratory of Industrial Chemistry, P.O.Box 6100, FIN-02015 HUT, Finland.

to describe the reaction kinetics under a wide range of conditions. It has been postulated that the activity of the catalyst depends also on the solution's microenvironment in the pores. The strength of the active site, the proton H^+ , may be influenced by the solvents. An attempt to take this phenomenon into account has been the use of the Hildebrand solubility parameter to characterize the influence of the reaction medium on the catalytic activity. The parameter is directly related to the swelling and to the accessibility of the active sites [7]. Another approach has been to describe the equilibrium between the polymer phase and the liquid phase through the extended Flory-Huggins theory [8].

In the earlier study [9] we carried out a large number of batch reactor experiments varying the reagent's initial molar ratio (methanol/isoamylenes: $R_{IA} = 0.2-2.0$ and methanol/2M1B: $R_{1b} = 1.0$) and temperature (333–353 K). We also tested three mechanisms in the formation reaction of TAME: homogeneous, Eley-Rideal type and Langmuir-Hishelwood type. From the tested models the Eley-Rideal type model described the experimental results best. In this mechanism it was assumed that only the alcohol and the product ether adsorb to the catalyst and the isoamylenes react from the surrounding liquid phase. However, in this model the isomerization reaction is assumed to happen noncatalytically. Fig. 2 shows the other fundamental weakness of the model, in cases where isoamylenes were fed in large excess (5:1) to methanol, the model describes the initial rate and equilibrium rather well, but the rise in the reaction rate to TAME when methanol molar fraction becomes smaller than 0.1 is not predicted satisfactorily by the previous model. Being linear in character the model is not able to describe the weak S-curve shown by the experimental points in Fig. 2.

In the previous study [10] of simultaneous isomerization and etherification of isoamylenes it was observed that the different alcohols (methanol, ethanol, and 1-propanol) affected the initial isomerization rate but not the initial etherification rate. Measurements carried out with different molar ratios of the reagents showed that with ethanol the initial isomerization and the initial etherification rates were equal until the lowest molar ratio (0.2) was reached. Also the initial reaction rates had a constant value at stoichiometric or higher ethanol/2M1B

molar ratios. A new model was developed to explain the results for TAE. In this model the adsorption is not competitive, but alcohol adsorbs first and then alkenes and ether adsorb to the same site. This model described the experimental results better at low alcohol contents.

In this work, we present the results of the simultaneous isomerization and etherification of isoamylenes measured with different initial methanol/alkene molar ratios. These results give important information on the behavior of the etherification and isomerization reactions. Several simple and precise kinetic correlations are tested to explain all the obtained results of the experiments carried out in this and earlier studies [9].

2 Experiments

The effect of feed MeOH/2M1B molar ratio on the initial isomerization and etherification rates was studied at a temperature of 333 K in a batch reactor. Experiments were carried out both without and with solvent (isopentane or isooctane) in order to vary the alcohol molar fraction correspondingly. The initial reaction rates for etherification and isomerization were obtained from the slopes of the lines of formed TAME and 2M2B (moles) plotted as a function of contact time (h·g cat.). Additional data has been published earlier in [9].

2.1 Reactor

The initial reaction rate experiments were carried out in a batch reactor (80 cm³ stainless steel). The reaction mixture was stirred magnetically. The catalyst was placed in a metal gauze basket (60 mesh, 2 cm³), that also worked as a mixing baffle in the reactor. The temperature (333 K) was controlled within ± 0.2 K by immersing the reactor in a thermostated water bath. The pressure was kept constant at 0.7 – 0.8 MPa, with an accuracy of 0.03 MPa, to guarantee a liquid-phase operation at all temperatures. Samples were withdrawn from the reactor every 15 minutes. Detailed description of the experimental set-up and procedure is given elsewhere [9].

2.2 Analytical Methods

A Hewlett-Packard gas chromatograph 5890 Series II, equipped with a flame ionization detector, was used for the analysis. The compounds were separated in a 60 m \times 0.258 mm glass capillary column HP-1 with a film thickness of 1.0 μ m (Hewlett Packard). All compounds were calibrated in order to obtain quantitative results. The reproducibility of the analysis was ± 3 %.

2.3 Catalyst

The catalyst used was a commercial, strong cation exchange resin, Amberlyst 16 W (Rohm & Haas), which exchange

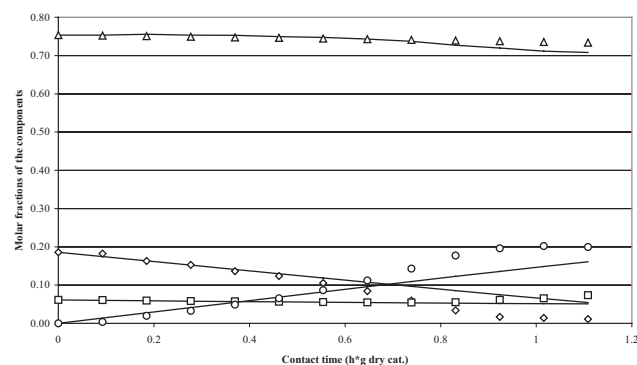


Figure 2. Simulated (—) and experimental molar fractions of the components (o) TAME, (□) 2M1B, (Δ) 2M2B, (◇) MeOH. Experiment carried out with $R_{IA} = 0.2$ at 343 K.

capacity is 5.0 meq/g dry catalyst, and cross-linking level is 12 wt.-%. The catalyst particles were pre-treated as described in [9]. The catalyst was sieved, and a particle size of 0.3–0.6 mm was used in the experiments. The catalyst was changed after each run. After the runs the catalyst was dried and weighed. All rate calculations are based on the amount of dry catalyst. The amount of dry catalyst used in the experiments varied between 0.2259 and 0.4144 g.

2.4 Reactants and Solvents

The reagents used were methanol (MeOH, Riedel-de Haën, >99.8 %) and 2-methyl-1-butene (2M1B, 99 wt.-%, Aldrich). In some experiments, the reagents were diluted with unreactive hydrocarbons, isopentane (Fluka Chemie, p.a.) or isooctane (Riedel-de Haën, p.a.).

3 Results and Discussion

3.1 Initial Reaction Rates

In order to study the effect of methanol/alkene initial molar ratio on the initial reaction rates, measurements were made with different MeOH/2M1B ratios. The results of the experiments carried out at 333 K are presented in Tab. 1. According to the table initial reaction rates for etherification and isomerization increase as the MeOH/2M1B mole ratio decreases and the ratio of etherification and isomerization rate is 2–3 until at lowest initial MeOH/2M1B mole ratio 0.2, where the isomerization rate increases significantly. At MeOH/2M1B mole ratio 0.2 the isomerization reaction rate is twice as high as the etherification reaction rate (for conversions see Figs. 3 a) and b). When solvents have been used, both rates are considerably lower.

Table 1. Results of initial reaction rate measurements with varying initial MeOH/2M1B-ratios.

Initial feed conditions			Initial rates mol/(h ^g dry cat.)		Ratio of rates Ether/Isom
MeOH/ 2M1B	MeOH mol-%	Solvent mol-% (¹ isopentane) (² isooctane)	Etherifica- tion	Isomeriza- tion	
0.19	16	0	0.149	0.376	0.4
0.22	18	0	0.153	0.322	0.5
0.50	18	47 ¹	0.041	0.017	2.3
0.54	31	12 ²	0.113	0.075	1.5
0.61	38	0	0.183	0.102	1.8
0.85	54	0	0.121	0.045	2.7
1.17	48	0	0.114	0.045	2.5
1.13	35	33 ²	0.033	0.013	2.5
4.05	80	0	0.086	0.027	3.2

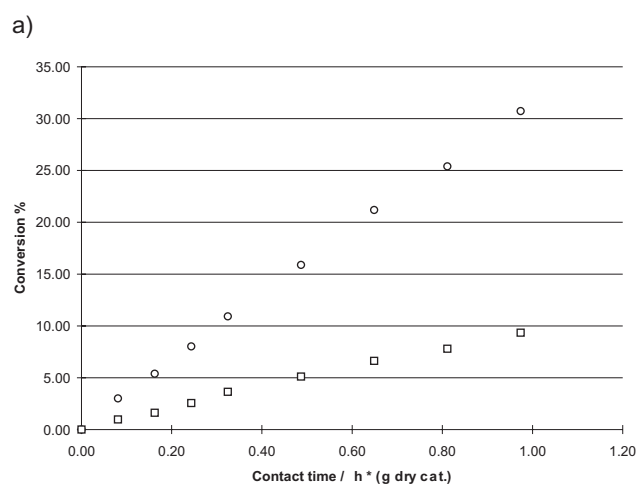


Figure 3a. Conversion of 2M1B to TAME (o) and to 2M2B (□) as a function of contact time. Experiment carried out with $R_{Tb} = 4.0$ at 333 K.

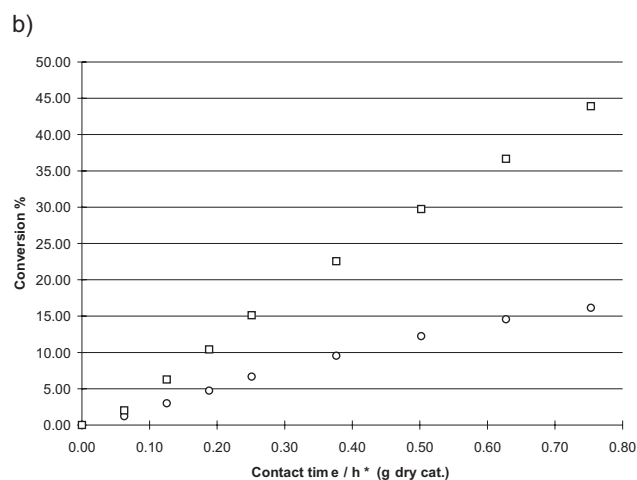


Figure 3b. Conversion of 2M1B to TAME (o) and to 2M2B (□) as a function of contact time. Experiment carried out with $R_{Tb} = 0.2$ at 333 K.

Fig. 4 shows, how the ratio of isomerization rates (isomerization rate/isomerization rate at stoichiometric conditions) increases exponentially with the molar fraction of 2M1B in the feed reaction mixture. The ratio of rates varies between 0.2 at $X_{1b} = 0.2$ and 8 at $X_{1b} = 0.8$.

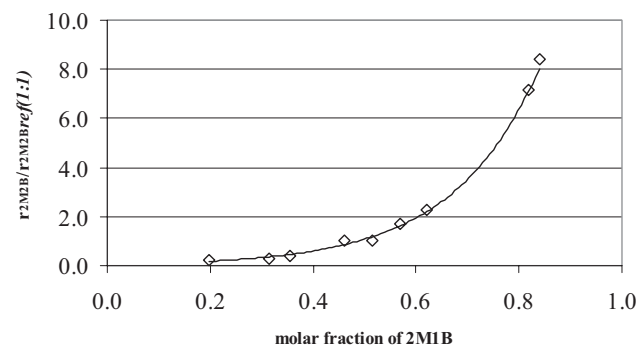


Figure 4. Ratio of initial isomerization rate and initial isomerization rate at stoichiometric conditions as a function of the initial molar fraction of 2M1B in the feed.

3.2 Simple Kinetic Models

Several simple correlations based on different mechanistic assumptions were tested against the batch reactor data. Different correlations and their mechanistic base are presented in Tab. 2. In deriving all the equations it was assumed that the surface reaction is the rate determining step and that alcohol is the dominant molecule to adsorb [7]. As a first approximation this assumption seems to be justified based on the adsorption measurements of Oktar et al. [11]. According to them the adsorption equilibrium constants of alcohols on Amberlyst 15 catalyst are about two orders of magnitude greater than the adsorption equilibrium constants of C4, C5 i-alkenes, MTBE and TAME. The fraction of vacant sites has also been neglected. The driving force factors including the equilibrium constants in the equations are the following¹⁾:

$$DF_1 = \frac{a_{TAME}}{a_{1b} a_M K_1} \quad (1)$$

$$DF_2 = \frac{a_{TAME}}{a_{2b} a_M K_2} \quad (2)$$

$$DF_3 = \frac{a_{2b}}{a_{1b} K_3} \quad (3)$$

3.3 Equilibrium Constants

The equilibrium compositions have been published by Rihko et al. [3] and more precisely by Rihko-Struckmann et al. [12]. The temperature dependencies of the equilibrium constants are presented in Eqs. (4)–(6) (Wilson method of activity coefficients calculation):

$$K_1 = \exp(-8.74435 + 4142.069/T) \quad (4)$$

$$K_2 = \exp(-8.24371 + 3219.118/T) \quad (5)$$

$$K_3 = K_1/K_2 \quad (6)$$

3.4 Procedure

Earlier data presented in [9] and some of the new data presented here sum up to total 359 observation points. The data points of the two extreme experiments, where the initial

Table 2. Simple kinetic models and their mechanistic base.

Model	Mechanism	Rate equations
1	IA* + MeOH** ↔ TAME* + 2* or IA* + MeOH** ↔ TAME** + *	$r_{TAME} = \frac{k_1 a_{1b}}{\sqrt{a_M}} (1 - DF_1) + \frac{k_3 a_{2b}}{\sqrt{a_M}} (1 - DF_2)$ $r_{ISOM} = \frac{k_5 a_{1b}}{\sqrt{a_M}} (1 - DF_3)$
2	IA* + MeOH* ↔ TAME* + * or IA* + MeOH* ↔ TAME**	$r_{TAME} = \frac{k_1 a_{1b}}{a_M} (1 - DF_1) + \frac{k_3 a_{2b}}{a_M} (1 - DF_2)$ $r_{ISOM} = \frac{k_5 a_{1b}}{a_M} (1 - DF_3)$
3	IA** + MeOH* ↔ TAME* + 2* or IA** + MeOH* ↔ TAME** + *	$r_{TAME} = \frac{k_1 a_{1b}}{a_M^2} (1 - DF_1) + \frac{k_3 a_{2b}}{a_M^2} (1 - DF_2)$ $r_{ISOM} = \frac{k_5 a_{1b}}{a_M^2} (1 - DF_3)$
4	IA ₂ * + 2MeOH** ↔ 2TAME** + *	$r_{TAME} = \frac{k_1 a_{1b}^2}{\sqrt{a_M}} (1 - DF_1) + \frac{k_3 a_{2b}^2}{\sqrt{a_M}} (1 - DF_2)$ $r_{ISOM} = \frac{k_5 a_{1b}^2}{\sqrt{a_M}} (1 - DF_3)$
5	IA ₂ * + 2MeOH* ↔ 2TAME* + *	$r_{TAME} = \frac{k_1 a_{1b}^2}{a_M} (1 - DF_1) + \frac{k_3 a_{2b}^2}{a_M} (1 - DF_2)$ $r_{ISOM} = \frac{k_5 a_{1b}^2}{a_M} (1 - DF_3)$
6	IA ₂ * + 2 MeOH* + * ↔ 2 TAME**	$r_{TAME} = \frac{k_1 a_{1b}^2}{a_M^2} (1 - DF_1) + \frac{k_3 a_{2b}^2}{a_M^2} (1 - DF_2)$ $r_{ISOM} = \frac{k_5 a_{1b}^2}{a_M^2} (1 - DF_3)$
		$DF_1 = \frac{a_{TAME}}{a_{1b} a_M K_1} \quad DF_2 = \frac{a_{TAME}}{a_{2b} a_M K_2} \quad DF_3 = \frac{a_{2b}}{a_{1b} K_3}$

methanol/2M1B molar ratio was 0.2, were not included in this regression analysis. The estimation was carried out with the KINFIT estimation program [13] by minimizing with the Levenberg-Marquardt method the weighted sum of residual squares (WSRS) between the experimental and calculated compositions (mol) in the outlet of the reactor. Weight factor (Wi) 1 was used for all compounds.

$$WSRS = \sum (n_{exp} - n_{calc})^2 w_i \quad (7)$$

The activity coefficients were calculated with the Wilson method, the parameters have been presented in a recent study by Rihko-Struckmann et al. [12]. The estimated parameters were the rate coefficients k₁, k₃ and k₅ at 343 K and their Arrhenius-type activation energies E₁, E₂ and E₃, respectively.

3.5 Results of Calculations with Simple Correlations

From the simple kinetic models presented in Tab. 2, model 3 has the smallest residual sum of squares (RSS = 0.683) and

1) List of symbols at the end of the paper.

model 4 the greatest (RSS = 0.887). The second best model is model 2 (RSS = 0.759), also suggested earlier by Oost and Hoffmann [14]. The estimated parameters of the models 2 and 3 are presented in Tab. 3. The parameters are well identified, their standard errors ranging from 0.5 to 8.9 %. Also the obtained activation energies fell into a satisfactory range:

Table 3. Results of parameter estimation. Simple models 2 and 3.

Model 2				95 % confidence limits	
Parameter	Value	Standard Error	S.E. %	Lower	Upper
k_1	0.061312	0.000842	1.4	5.97E-02	6.30E-02
E_1	76980.5	1650	2.1	73745.14	80215.95
k_3	0.024909	0.000159	0.6	2.46E-02	2.52E-02
E_2	85715.3	863	1.0	84023.98	87406.69
k_5	0.025086	0.00108	4.3	2.30E-02	2.72E-02
E_3	89843.7	5130	5.7	79780.94	99906.36
Model 3					
k_1	0.047452	0.00059	1.2	4.63E-02	4.86E-02
E_1	75489.7	1510	2.0	72526.99	78452.39
k_3	0.018971	0.000103	0.5	1.88E-02	1.92E-02
E_2	85379.2	7610	8.9	83887.51	86870.84
k_5	0.019711	0.000798	4.0	1.81E-02	2.13E-02
E_3	87856.8	4860	5.5	78340.55	97373.06

from 75.5 kJ/mol for the etherification of 2-methyl-1-butene to 89.8 kJ/mol for the isomerization of 2-methyl-1-butene. These values agree well with the values published in the literature. In our earlier study [9] the activation energy was determined to be 81.6 kJ/mol for the isomerization and 72.6 kJ/mol for the etherification of 2M1B to TAME and 94.1 kJ/mol for the etherification of 2M2B. Piccoli and Lovisi [15] reported activation energies of 84.8 and 92.8 kJ/mol for the etherification of 2M1B and 2M2B, respectively. In studies where the isoamylenes have been lumped together, values of activation energy of 81.1 kJ/mol [16], 89.5 kJ/mol [14] and 94.0 kJ/mol [17] have been reported for the etherification.

These simple models can be used in preliminary calculations when designing a reactor for etherification, but since accurate adsorption equilibrium measurements have been published [11], we will carry out a more precise kinetic study in the following section.

3.6 Precise Correlations with Adsorption Equilibrium Constants

Four correlations based on different mechanisms were tested against the data and the adsorption measurements of Oktar et al. [11] were used to express the relative adsorption

phenomena in the system. Three of these models and their derivations have been presented in our earlier studies. The Eley-Rideal type (adsorption of alcohol and ether) and Langmuir-Hishelwood type (adsorption of all components) models were presented in [9]. The modified Eley-Rideal mechanism (adsorption of alcohol first and the alkene adsorption to the same site) was presented in [10]. Therefore, their derivations are not repeated here. The fourth model is a so-called Lewis-Bronsted model [18]. In this model it is assumed that the catalyst contains two different kinds of acidic sites, the Bronsted-proton H^+ and the Lewis $:O:$ in its SO_3H -groups. The mechanism of etherification is presented in Fig. 5.

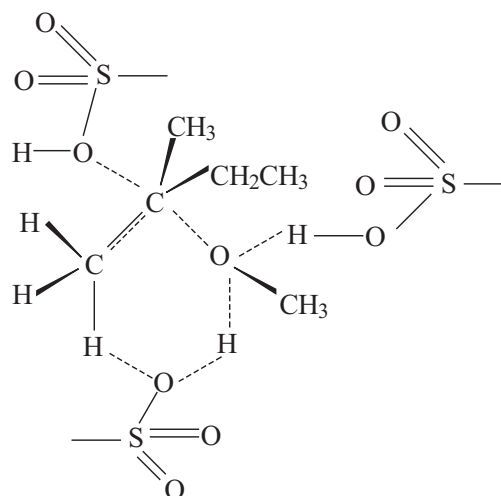


Figure 5. Proposed Bronsted-Lewis mechanism according to Tejero *et al.* [18].

Derivation proceeds as follows:

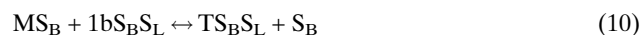
Alcohol molecule adsorbs to a Bronsted site (H^+):



2M1B adsorbs to one Bronsted and to one Lewis site ($:O:$):



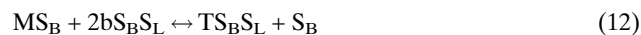
Adsorbed methanol and 2M1B yield TAME in etherification:



Adsorbed 2M1B can isomerize to 2M2B:



Adsorbed methanol and 2M2B yield TAME in etherification:



Finally TAME and 2M2B desorb:



The rate limiting steps for the etherification and for the isomerization reactions are assumed to be the surface reactions, Eqs. (10), (11), and (12). Using these assumptions and Eqs. (8)–(14), the rate equations for etherification, Eq. (15) and isomerization, Eq. (16) can be written as follows:

$$r_{ETHER} = k_1 \theta_{M,B} \theta_{1b,B} \theta_{1b,L} - k_2 \theta_{T,B} \theta_{T,L} \theta_{SB} + k_3 \theta_{M,B} \theta_{2b,B} \theta_{2b,L} - k_4 \theta_{T,B} \theta_{T,L} \theta_{SB} \quad (15)$$

$$r_{ISOM} = k_5 \theta_{1b,B} \theta_{1b,L} - k_6 \theta_{2b,B} \theta_{2b,L} \quad (16)$$

The surface concentrations of the species θ_i can be described with the Langmuir isotherm, where K_i is the adsorption equilibrium constant and a_i is the activity of component i :

$$\theta_i = \frac{K_i a_i}{1 + \sum K_i a_i} \quad (17)$$

The site balance for Bronstedt sites:

$$\theta_{M,B} + \theta_{1b,B} + \theta_{2b,B} + \theta_{T,B} + \theta_{SB} = 1 \quad (18)$$

$$K_M a_M \theta_{SB} + \frac{K_{1b} a_{1b} \theta_{SB} \theta_{SL}}{\theta_{1b,L}} + \frac{K_{2b} a_{2b} \theta_{SB} \theta_{SL}}{\theta_{2b,L}} + \frac{K_T a_T \theta_{SB} \theta_{SL}}{\theta_{T,L}} + \theta_{SB} = 1 \quad (19)$$

$$\theta_{SB} = \frac{1}{K_M a_M + K_{1b} a_{1b} \frac{\theta_{SL}}{\theta_{1b,L}} + K_{2b} a_{2b} \frac{\theta_{SL}}{\theta_{2b,L}} + K_T a_T \frac{\theta_{SL}}{\theta_{T,L}} + 1} \quad (20)$$

The site balance for Lewis sites:

$$\theta_{1b,L} + \theta_{2b,L} + \theta_{T,L} + \theta_{SL} = 1 \quad (21)$$

$$\frac{K_{1b} a_{1b} \theta_{SB} \theta_{SL}}{\theta_{1b,B}} + \frac{K_{2b} a_{2b} \theta_{SB} \theta_{SL}}{\theta_{2b,B}} + \frac{K_T a_T \theta_{SB} \theta_{SL}}{\theta_{T,B}} + \theta_{SL} = 1 \quad (22)$$

$$\theta_{SL} = \frac{1}{K_{1b} a_{1b} \frac{\theta_{SB}}{\theta_{1b,B}} + K_{2b} a_{2b} \frac{\theta_{SB}}{\theta_{2b,B}} + K_T a_T \frac{\theta_{SB}}{\theta_{T,B}} + 1} \quad (23)$$

But rather than applying separate site balances in deriving the kinetic equations, we assume from the scheme presented in Fig. 5, that there is an equivalent amount of unoccupied

Bronstedt and Lewis sites. Therefore we will apply the following equality in the equations:

$$\theta_{SL} = \theta_{SB} \quad (24)$$

For etherification:

$$r_{ETHER} = k_1 K_M a_M \theta_{SB} K_{1b} a_{1b} \theta_{SB} \theta_{SL} - k_2 K_T a_T \theta_{SB}^2 \theta_{SL} + k_3 K_M a_M \theta_{SB} K_{2b} a_{2b} \theta_{SB} \theta_{SL} - k_4 K_T a_T \theta_{SB}^2 \theta_{SL} \quad (25)$$

$$r_{ETHER} = \frac{k_1 K_M a_M K_{1b} a_{1b} - k_2 K_T a_T + \frac{k_3 K_M a_M K_{2b} a_{2b} - k_4 K_T a_T}{K_{2b} a_{2b} \frac{\theta_{SL}}{\theta_{2b,L}} + K_T a_T \frac{\theta_{SL}}{\theta_{T,L}} + 1}}{(K_M a_M + K_{1b} a_{1b} \frac{\theta_{SL}}{\theta_{1b,L}} + \frac{k_3 K_M a_M K_{2b} a_{2b} - k_4 K_T a_T}{K_{2b} a_{2b} \frac{\theta_{SL}}{\theta_{2b,L}} + K_T a_T \frac{\theta_{SL}}{\theta_{T,L}} + 1})^3} \quad (26)$$

Again based on the scheme, the fraction of vacant Lewis sites is 1/3 and the fractions of sites occupied by the alkenes or TAME are 2/3, so the ratios in the denominator equal 1/2. Taking along the equilibrium constants we finally get:

$$r_{ETHER} = \frac{k_1 K_M a_M K_{1b} a_{1b} (1 - \frac{a_T}{K_1 a_M a_{1b}}) + \frac{k_3 K_M a_M K_{2b} a_{2b} (1 - \frac{a_T}{K_2 a_M a_{2b}})}{\frac{K_{1b} a_{1b} + K_{2b} a_{2b} + K_T a_T + 1}{2}}}{(K_M a_M + \frac{K_{1b} a_{1b} + K_{2b} a_{2b} + K_T a_T + 1}{2})^3} \quad (27)$$

For isomerization:

$$r_{ISOM} = k_5 K_{1b} a_{1b} \theta_{SB} \theta_{SL} - k_6 K_{2b} a_{2b} \theta_{SB} \theta_{SL} \quad (28)$$

$$r_{ISOM} = \frac{k_5 K_{1b} a_{1b} (1 - \frac{a_{2b}}{K_3 a_{1b}})}{(K_M a_M + \frac{K_{1b} a_{1b} + K_{2b} a_{2b} + K_T a_T + 1}{2})^2} \quad (29)$$

For parameter estimation purposes, the equations were divided with K_M^3 and it was assumed that the term $1/K_M^3$ was small compared to other terms in the denominator:

$$r_{ETHER} = \frac{k'_1 a_M a_{1b} (1 - \frac{a_T}{K_1 a_M a_{1b}}) + k'_3 a_M a_{2b} (1 - \frac{a_T}{K_2 a_M a_{2b}})}{(a_M + \frac{1}{2} \frac{K_{1b} a_{1b} + K_{2b} a_{2b} + K_T a_T}{K_M})^3} \quad (30)$$

$$r_{ISOM} = \frac{k'_5 a_{1b} (1 - \frac{a_{2b}}{K_3 a_{1b}})}{(a_M + \frac{1}{2} \frac{K_{1b} a_{1b} + K_{2b} a_{2b} + K_T a_T}{K_M})^2} \quad (31)$$

where $k'_1 = k_1 \frac{K_{1b}}{K_M^2}$, $k'_3 = k_3 \frac{K_{2b}}{K_M^2}$ and $k'_5 = k_5 \frac{K_{1b}}{K_M^2}$.

This and the other correlations are presented in Tab. 4.

Table 4. Precise correlations and their mechanistic base.

Mechanism	$r_{\text{ETHER}} =$	$r_{\text{ISOM}} =$
Eley-Rideal Adsorption of alcohol and ether	$\frac{k_1 a_M a_{1b} \left(1 - \frac{a_T}{K_1 a_M a_{1b}}\right) + k_3 a_M a_{2b} \left(1 - \frac{a_T}{K_2 a_M a_{2b}}\right)}{\left(\frac{K_T}{K_M} a_T + a_M\right)}$	$k_5 a_{1b} \left(1 - \frac{a_{2b}}{K_3 a_{1b}}\right)$
Langmuir-Hinshelwood Adsorption of all components	$\frac{k_1 \frac{K_{1b}}{K_M} a_M a_{1b} \left(1 - \frac{a_T}{K_1 a_M a_{1b}}\right) + k_3 \frac{K_{2b}}{K_M} a_M a_{2b} \left(1 - \frac{a_T}{K_2 a_M a_{2b}}\right)}{\left(\frac{K_T}{K_M} a_T + a_M + \frac{K_{1b}}{K_M} a_{1b} + \frac{K_{2b}}{K_M} a_{2b}\right)^2}$	$\frac{k_5 \frac{K_{1b}}{K_M} a_{1b} \left(1 - \frac{a_{2b}}{K_3 a_{1b}}\right)}{\left(\frac{K_T}{K_M} a_T + a_M + \frac{K_{1b}}{K_M} a_{1b} + \frac{K_{2b}}{K_M} a_{2b}\right)}$
Modified Eley-Rideal Adsorption of olefin and ether to the same site	$\frac{k'_1 a_M a_{1b} \left(1 - \frac{a_T}{K_1 a_M a_{1b}}\right) + k'_3 a_M a_{2b} \left(1 - \frac{a_T}{K_2 a_M a_{2b}}\right)}{\left(\frac{K_{1b}}{K_T} a_{1b} + \frac{K_{2b}}{K_T} a_{2b} + a_T\right) (1 + K_M a_M)}$	$\frac{k'_5 a_{1b} \left(1 - \frac{a_{2b}}{K_3 a_{1b}}\right)}{\left(\frac{K_{1b}}{K_T} a_{1b} + \frac{K_{2b}}{K_T} a_{2b} + a_T\right)}$
Lewis-Bronstedt Adsorption of alcohol to Bronstedt sites Adsorption of olefin and ether to one Bronstedt and one Lewis site	$\frac{k'_1 a_M a_{1b} \left(1 - \frac{a_T}{K_1 a_M a_{1b}}\right) + k'_3 a_M a_{2b} \left(1 - \frac{a_T}{K_2 a_M a_{2b}}\right)}{\left(a_M + \frac{1K_{1b}}{2K_M} a_{1b} + \frac{1K_{2b}}{2K_M} a_{2b} + \frac{1K_T}{2K_M} a_T\right)^3}$	$\frac{k'_5 a_{1b} \left(1 - \frac{a_{2b}}{K_3 a_{1b}}\right)}{\left(a_M + \frac{1K_{1b}}{2K_M} a_{1b} + \frac{1K_{2b}}{2K_M} a_{2b} + \frac{1K_T}{2K_M} a_T\right)^2}$

3.7 Adsorption Equilibrium Constants

Oktar et al. [11] measured the adsorption equilibrium constants of reactants and products in MTBE, ETBE and TAME production on Amberlyst 15 with packed bed moment technique. Their results for single tracers are presented in Tab. 5. The effect of alcohol presence on the adsorption equilibrium constants of i-alkenes was studied with ethanol-pretreated catalyst and 2M2B. The results showed that the adsorption equilibrium constant of 2M2B on a pretreated catalyst was about three times greater than the corresponding value obtained on fresh catalyst. This might be due to the swelling of the catalyst, which opens more micropores and consequently more acidic sites, in other words, more surface area becomes available for alkene adsorption. Because in our system, there was always alcohol present we assumed that we could multiply the adsorption equilibrium constants of alkenes and TAME from Tab. 5 with three. Furthermore, the values were divided with the adsorption constant of methanol or TAME (Tab. 6).

Table 5. Results of adsorption equilibrium constant measurements by Oktar et al. [11].

Temperature / K	MeOH	2M1B	2M2B	TAME
323	9700	133	94	56
340	8800	63	68	37
358	7600	40	42	32
Adsorption enthalpy kJ/mol	-6.7	-37.2	-26.8	-18.1

Table 6. Ratios of adsorption equilibrium constants at different temperatures.

Ratio	323 K	340 K	358 K
K_{1b}/K_M	0.0424	0.0222	0.0163
K_{2b}/K_M	0.0300	0.0239	0.0171
K_T/K_M	0.0179	0.0130	0.0130
K_{1b}/K_T	2.375	1.703	1.250
K_{2b}/K_T	1.679	1.838	1.313

We calculated the temperature dependencies of these ratios to be the following:

$$\frac{K_{1b}}{K_M} = \exp(-13.0304 + 3171.451/T) \quad (32)$$

$$\frac{K_{2b}}{K_M} = \exp(-9.22212 + 1852.525/T) \quad (33)$$

$$\frac{K_T}{K_M} = \exp(-7.32796 + 1050.648/T) \quad (34)$$

$$\frac{K_{1b}}{K_T} = \exp(-5.70243 + 2120.803/T) \quad (35)$$

$$\frac{K_{2b}}{K_T} = -0.0011 * T^2 + 0.7397 * T - 122.32 \quad (36)$$

These dependencies were used as fixed values when estimating the rate parameters of different kinetic models.

3.8 Results of Parameter Estimation

Parameter estimation of different models was carried out with KINFIT, the estimated parameters were the rate parameters k_1 , k_3 and k_5 and their activation energies. The activation energies were obtained from the Arrhenius type temperature dependence. In order to avoid strong correlation between the parameters, 333 K was selected as reference temperature:

$$k = A_{ref} e^{-zE} \quad (37)$$

where A_{ref} is defined as $A_0 \exp(-E/RT_{ref})$ and z as $1/8.314 * (1/T - 1/T_{ref})$

The regression analysis was carried out against all available batch reactor data, including the two experiments, where the initial methanol/isoamylenol molar ratio was 0.2. Total number of observation points was therefore 375. The results of regression analysis are presented in Tab. 7.

According to the statistics, the Lewis-Bronstedt model has the smallest residual sum of squares (1.062) and the modified Eley-Rideal the largest (1.673). The second best model is Langmuir-Hinshelwood (1.227). These results are thus in line with those obtained with the simple models, where the mechanism based on three sites gave the best fit. No significant correlations between the parameters were observed. The parameters of the models were rather well identified in all the cases, standard errors ranged between 0.5 and 41 %. The largest errors were obtained for the activation energy of isomerization, 7.3 % with Langmuir-Hinshelwood and 41 % with modified Eley-Rideal. The obtained activation energies for etherification are again in satisfactory range (75.9–103.4 kJ/mol) for all the other models but modified Eley-Rideal. With modified Eley-Rideal they are slightly too small (53.0–70.6 kJ/mol). However, it must be noted that the obtained activation energies for the isomerization fell not to a satisfactory range with all the other models (16.0–37.6 kJ/mol) but Langmuir-Hinshelwood (70.7 kJ/mol). With stoichiometric feed the obtained activation energy for isomerization has been determined to be 81.6 kJ/mol [9]. So the results seem to support the Langmuir-Hinshelwood model most strongly. Figs. 6–9 show the estimated amounts of TAME (mol) with different models as a function of the observed amounts of TAME (mol). From the figures it can be seen, that the most severe deviations occur with both two Eley-Rideal type models. The Lewis-Bronstedt model gives the smallest deviations, but it severely underestimates some points, whereas Langmuir-Hinshelwood severely overestimates a few points.

Karinen et al. [19] compared the activities of Amberlyst 35 (capacity 5.2 mmol/g_{cat.}) and the polyethylene based fiber catalyst Smopex-101 (capacity 3.0 mmol/g_{cat.}) in the formation reaction of TAME. Amberlyst 35 showed a higher activity for ether formation than Smopex-101 at 80 °C. This might be an indication that the mechanism indeed requires two or more acidic groups to proceed. Because the density of the acidic

centers is greater in a typical macroreticular ion exchange resin than in the fiber catalyst the reaction rate is consequently faster with A35 than with the fiber catalyst.

However, the Lewis-Bronstedt mechanism presented in Fig. 5 represents a structure of high energy and requires a

Table 7. Results of parameter estimation. Precise correlations.

Eley-Rideal		Residual sum of squares	1.438841	95 % confidence limits	
Parameter	Value	Standard Error	S.E. %	Lower	Upper
k_1	0.0384	0.0010	2.6	0.0364	0.0403
E_1	73177	2187	3.0	68890	77463
k_3	0.0126	0.0002	1.5	0.0122	0.0129
E_2	88304	1248	1.4	85858	90750
k_5	0.0289	0.0014	4.7	0.0263	0.0316
E_3	37553	5660	15	26460	48646
Langmuir-Hinshelwood		Residual sum of squares	1.226933	95 % confidence limits	
Parameter	Value	Standard Error	S.E. %	Lower	Upper
k_1	1.3071	0.0177	1.4	1.2723	1.3418
E_1	84614	1631	1.9	81418	87811
k_3	0.3942	0.0050	1.3	0.3844	0.4040
E_2	103353	1083	1.0	101230	105476
k_5	0.7162	0.0341	4.8	0.6493	0.7831
E_3	70706	5161	7.3	60591	80821
Modified Eley-Rideal		Residual sum of squares	1.672817	95 % confidence limits	
Parameter	Value	Standard Error	S.E. %	Lower	Upper
k_1	575.8	15.8	2.7	544.8	606.7
E_1	53009	2255	4.3	48588	57430
k_3	200.8	3.0	1.5	195.0	206.7
E_2	70597	1260	1.8	68127	73068
k_5	0.0517	0.0026	5.1	0.0465	0.0568
E_3	15979	6541	40.9	3159	28799
Lewis-Bronstedt		Residual sum of squares	1.06201	95 % confidence limits	
Parameter	Value	Standard Error	S.E. %	Lower	Upper
k_1	0.0223	0.00003	0.1	0.0222	0.0224
E_1	75930	1196	1.6	73586	78275
k_3	0.0080	0.0001	1.1	0.0078	0.0081
E_2	85526	925	1.1	83714	87339
k_5	0.0177	0.0007	4.0	0.0163	0.0191
E_3	35887	4943	14	26199	45576

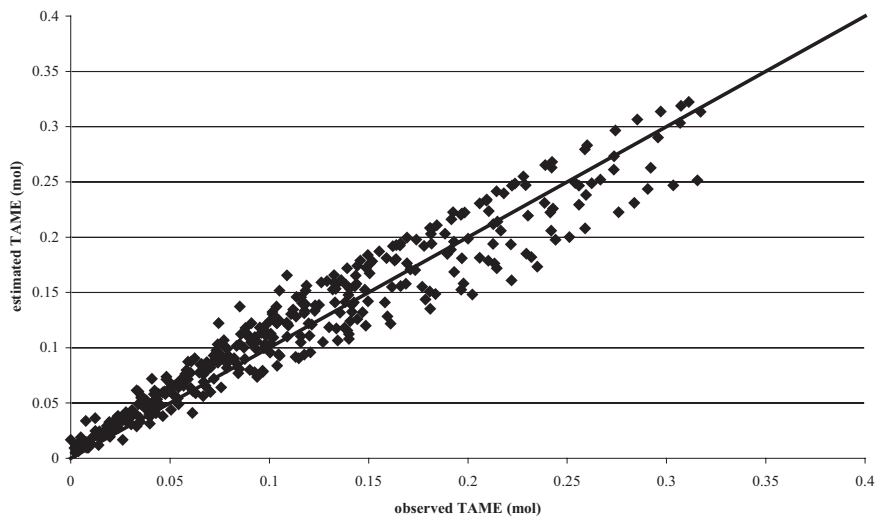


Figure 6. Observed and estimated amount of TAME (mol) with Langmuir-Hinshelwood model.

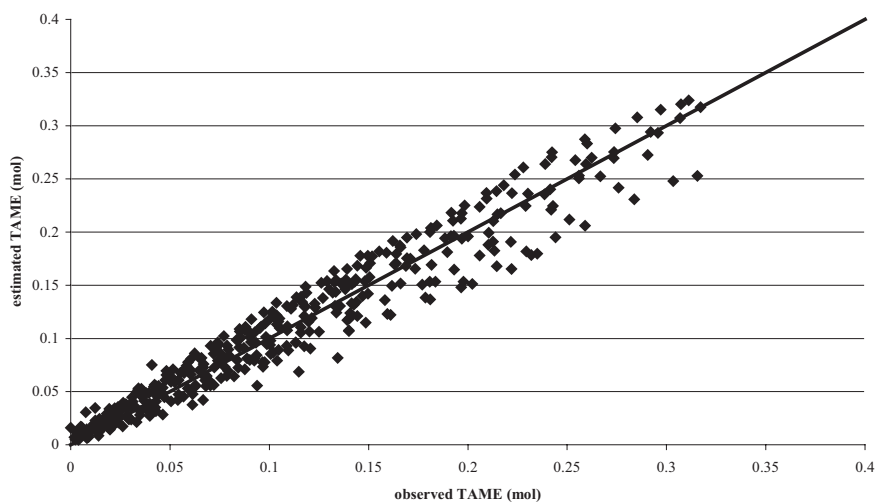


Figure 7. Observed and estimated amount of TAME (mol) with Lewis-Bronstedt model.

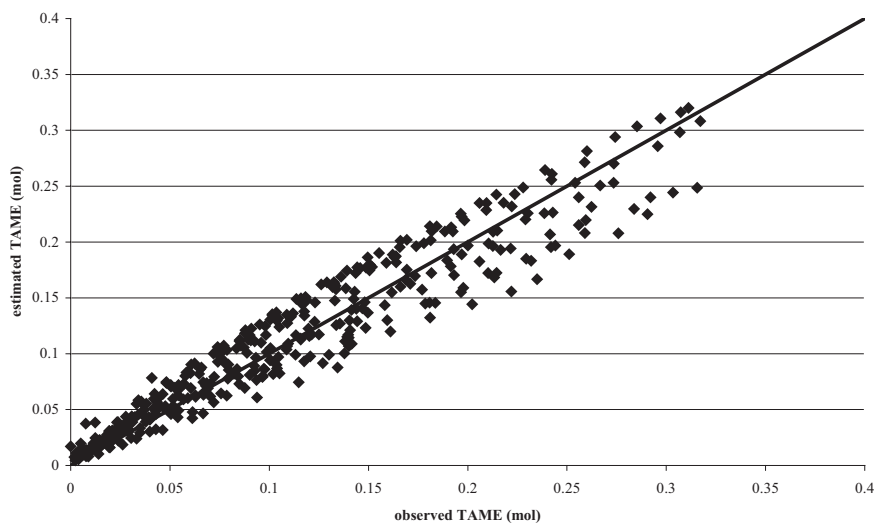


Figure 8. Observed and estimated amount of TAME (mol) with Eley-Rideal model.

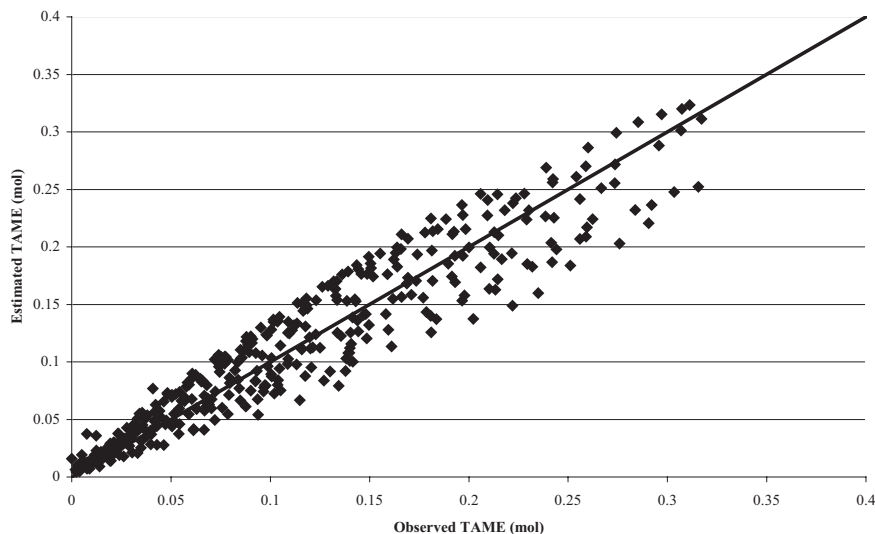


Figure 9. Observed and estimated amount of TAME (mol) with modified Eley-Rideal model.

pentamolecular collision. If the reactions were to occur in this way, it would require the sulfonic acid groups to be properly orientated at just right distances from the reacting molecules, rather like enzyme catalysis [20]. Actually, undirect evidence contradicts this mechanism. Kogelbauer et al. [20] studied the acid catalyzed hydrolysis of MTBE using p-toluenesulfonic acid as catalyst with NMR. The measurements showed protonation of methanol and MTBE by p-toluenesulfonic acid but no nucleophile-electrophile interaction of MTBE with p-toluenesulfonic acid methyl ester as a potential nucleophile.

Fig. 4 shows, how the isomerization rate depends exponentially of the molar fraction of 2M1B. This acceleration can be described with the following mathematical expression (acceleration of isomerization):

$$a.i. = 0.0006 \exp(6.148 \cdot X_{1b}) \quad (38)$$

When this factor is added into the equation describing the isomerization kinetics,

$$r_{ISOM} = \frac{k_5 \frac{K_{1b}}{K_M} a_{1b} (1 - \frac{a_{2b}}{K_3 a_{1b}}) a.i.}{(\frac{K_T}{K_M} a_T + a_M + \frac{K_{1b}}{K_M} a_{1b} + \frac{K_{2b}}{K_M} a_{2b})} \quad (39)$$

the residual sum of squares with the standard Langmuir-Hinshelwood model decreases from 1.227 to 0.840 (31.5 %). The parameters are also better identified, as their standard errors decrease (Tab. 8). Physicochemically this means, that the isomerization rate parameter k_5 depends on the composition of the reaction mixture, i.e., it is a function of the molar fraction of 2M1B in the mixture. Thus, according to the new experimental data presented in this study and based on the parameter estimation results we suggest a Langmuir-Hinshelwood type model corrected with the acceleration of isomerization for the TAME synthesis. The rate parameters of this model are presented in Tab. 8.

Table 8. Parameters of Langmuir-Hinshelwood model corrected with the acceleration of isomerization.

Parameter	Value	Standard Error	S.E. %	95 % confidence limits	
				Lower	Upper
k_1	0.9786	0.0194	2.0	0.9406	1.0165
E_1	101978	1650	1.6	98744	105211
k_3	0.4220	0.0042	1.0	0.4138	0.4302
E_2	101087	853	0.8	99415	102759
k_5	61.66	2.19	3.6	57.37	65.95
E_3	97210	4539	4.7	88314	106105

4 Summary

The effect of feed MeOH/2M1B molar ratio on the initial isomerization and etherification rates was studied at a temperature of 333 K in a batch reactor. Several kinetic models were tested against this new and the batch reactor data obtained earlier. Although the best fit was obtained with a model, whose mechanism was based on three active sites, the second best model of basic Langmuir-Hinshelwood type was considered to be more likely. A correction factor describing the acceleration of isomerization kinetics was added into the kinetic equations, which resulted in further improvement of the fit and even more precise values of the model parameters.

Acknowledgement

The financial support of the Academy of Finland through the Graduate School in Chemical Engineering (GSCE) is highly appreciated.

Received: August 8, 2001 [CET 1468]

Symbols used

A_0	[mol kg ⁻¹ s ⁻¹]	pre-exponential factor
a_i, x_i		activity of a component $i = \gamma_i x_i$
$a.i.$		acceleration factor of isomerization
DF		driving force factor
E	[J mol ⁻¹]	activation energy
k	[mol kg ⁻¹ s ⁻¹]	rate constant
K_i		adsorption equilibrium constant for a component i
K_j		reaction equilibrium constant for a reaction $j, j = 1-3$
$n_{i,calc}$	[mol]	amount of component i calculated by a model
$n_{i,exp}$	[mol]	amount of component i measured
r_i	[mol kg ⁻¹ s ⁻¹]	rate of reaction for component i
r_j		rate of reaction (Fig. 1), $j = 1-6$
R_{IA}		molar ratio of the reagents, methanol/isoamylene-mixture
R_{1b}		molar ratio of the reagents, methanol/2-methyl-1-butene
RSS		residual sum of squares
S		adsorption site on the catalyst
w_i		weight factor
x_i		molar fraction of component i

Abbreviations

WSRS	weighted sum of residual square
2M1B	2-methyl-1-butene
2M2B	2-methyl-2-butene
TAEE	tert-amyl ethyl ether, 2-ethoxy-2-methylbutane
TAME	tert-amyl methyl ether, 2-methoxy-2-methylbutane
MeOH	methanol

Greek symbols

γ_i	activity coefficient for component i
θ	fraction of sites

Indices

1b	2-methyl-1-butene
2b	2-methyl-2-butene
M	methanol
T	tert-amyl methyl ether
B	Bronstedt site H+
L	Lewis site :O:
ETHER	etherification
ISOM	isomerization

References

- [1] A. O. I. Krause, L. G. Hammarström, *Appl. Catal.* **1987**, *30*, 313.
- [2] L. K. Rihko, A. O. I. Krause, *Appl. Catal. A: General* **1993**, *101*, 283.
- [3] L. K. Rihko, J. A. Linnekoski, A. O. I. Krause, *J. Chem. Eng. Data* **1994**, *39*, 700.
- [4] J. Ignatius, H. Järvelin, P. Lindquist, *Hydrocarbon Proc.* **1995**, *74* (2), pp. 51.
- [5] W.-B. Su, J.-R. Chang, *Ind. Eng. Chem. Res.* **2000**, *39*, 4140.
- [6] A. W. Adamson, A. P. Gast, *Physical Chemistry of Surfaces*, 6th ed, Wiley, New York **1997**, p. 417.
- [7] C. Fite, M. Tejero, M. Iborra, F. Cunill, J. F., Izquierdo, *AIChE J.* **1998**, *44*, 2273.
- [8] M. Mazzotti, B. Neri, D. Gelosa, A. Kruglov, M. Morbidelli, *Ind. Eng. Chem. Res.* **1997**, *36*, 3.
- [9] L. K. Rihko, P. K. Kiviranta-Pääkkönen, A. O. I. Krause, *Ind. Eng. Chem. Res.* **1997**, *36*, 614.
- [10] J. A. Linnekoski, L. K. Rihko-Struckmann, P. K. Kiviranta-Pääkkönen, A. O. I. Krause, *Ind. Eng. Chem. Res.* **1999**, *38*, 4563.
- [11] N. Oktar, K. Mürtezaogly, T. Dogu, G. Dogu, *Can. J. Chem. Eng.* **1999**, *77*, 406.
- [12] L. K. Rihko-Struckmann, J. A. Linnekoski, O. S. Pavlov, A. O. I. Krause, *J. Chem. Eng. Data* **2000**, *45*, 1030.
- [13] J. Aittamaa, K. I. Keskinen, *KINFIT User Manual*, Helsinki University of Technology, Espoo **1998**.
- [14] C. Oost, U. Hoffmann, *Chem. Eng. Sci.* **1996**, *51*, 329.
- [15] R. L. Piccoli, H. R. Lovisi, *Ind. Eng. Chem. Res.* **1995**, *34*, 510.
- [16] S. Randriamahefa, R. Gallo, G. Raoult, P. Mulard, *J. Mol. Catal.* **1988**, *49*, 85.
- [17] W.-S. Hwang, J.-C. Wu, *J. Chin. Chem. Soc.* **1994**, *41*, 181.
- [18] J. Tejero, M. Cunill, M. Iborra, *J. Mol. Catal.* **1987**, *42*, 257.
- [19] R. S. Karinen, A. O. I. Krause, K. Ekman, M. Sundell, R. Peltonen, *Stud. Surf. Sci. Catal.* **2000**, *130*, 3411.
- [20] A. Kogelbauer, J. Reddick, D. Farcasiu, *J. Mol. Catal. A: Chem.* **1995**, *103*, 31.